JOURNAL OF MATERIALS SCIENCE 33 (1998) 4225–4234

Micromechanics of multiple cracking

Part II *Statistical tensile behaviour*

J. KULLAA
VTT Building Technology, P.O. Box 18071, FIN-02044 VTT, Finland
E-mail: jyrki.kullaa@vtt.fi

A computational model for fibre-reinforced brittle materials in tension is developed. The model includes multiple cracking and strain-hardening processes, as well as single fracture and strain softening. The composite behaviour is derived from a single-fibre analysis by integrating over all possible fibre locations and orientations. The single-fibre analysis is based on symmetry fibres satisfying the equilibrium condition. The result is a complete constitutive relation: stress–strain or stress–crack width curve, and a prediction of crack spacing. The model is an extension of the ACK theory by Aveston, Cooper and Kelly, as it can be used with discontinuous fibres with different distributions, as well as for analysing hybrid composites. Fibre orientation introduces additional phenomena, which are taken into account with simple models. It was seen that matrix spalling at the fibre exit point may have a considerable effect on the composite strain and the crack width. The effect of fibre aspect ratio on the failure mode was studied, and it was found that with an intermediate fibre diameter the composite fails by fibre pull-out in a multiple-cracking stage, resulting in a strain-hardening material with a high ductility. The proposed model was verified against experimental results of a strain-hardening material, called an engineered cementitious composite. The model can be used in tailoring new materials to meet certain requirements, or in studying the effects of micromechanical properties on the composite behaviour, including the crack width, crack spacing, post-cracking strength, ultimate strain, and ductility. The derived constitutive relationship can further be used in finite element analyses defining the behaviour perpendicular to the crack.

Nomenclature

A	= area of a sphere segment
A_f	= area of the fibre
A_m	= area of the matrix
A_m^i	= area of the matrix in pull-out analysis
$\hat{A}_m^i$	= area of the matrix in calculation of the composite stress
A_c	= unit area of the composite
d	= fibre diameter
E_f	= modulus of elasticity of the fibre
E_m	= modulus of elasticity of the matrix
E_c	= modulus of elasticity of an uncracked composite
k	= coefficient between spalled length and crack width
l	= segment length for an inclined fibre
l_f	= fibre length
l_{sp}	= matrix spalled length
N^i	= number of fibres of type i
P	= force in an inclined fibre at a crack
P_{aux}	= force perpendicular to a crack at the fibre bending point
$p(\theta)$	= probabilistic density function
Q	$= 1 + A_m E_m / A_f E_f$
s	= half of the segment length
T	= tensile force in the matrix
T_{aux}	= matrix proportion of P_{aux}
V_f	= fibre volume fraction
V_m	$= 1 - V_f$ = matrix volume fraction
w	= crack width
w_{sp}	= pull-out component of the crack width
ε_c	= composite strain
ε_m	= strain in the matrix
κ	= bond modulus
η_θ	= orientation efficiency factor
μ	= snubbing friction coefficient
φ	= fibre angle perpendicular to the crack due to matrix spalling
σ_c	= composite stress
σ_f	= stress in the fibre at a crack
σ_f'	= stress in an inclined fibre at a crack
σ_{fu}	= tensile strength of the fibre
σ_m	= stress in the matrix
σ_m^a	= aggregate bridging stress
σ_{mu}	= cracking stress of the matrix
θ	= inclination of a fibre from the perpendicular to a crack
θ_1, θ_2	= minimum and maximum inclinations of the fibre

0022–2461

τ_u = shear strength between fibre and matrix
τ_f = frictional shear stress between fibre and matrix

1. Introduction

The analysis of fibre-reinforced brittle materials, starting from the micromechanical material properties and leading to the finite element analysis of structures with complex geometries and loadings, falls roughly into three parts. First, the crack bridging analysis of a single fibre can be evaluated using the micromechanical material properties, which include the properties of the fibres, the matrix, and the interface. This theory has been developed and reported in Part I [1]. The second step is to perform a statistical analysis of all fibres with different locations and orientations, or different fibre types (hybrid) to obtain the macromechanical tensile behaviour. This step is important in the design or tailoring of new materials with high performance and low costs. The objective of the present work is to perform this second step. The results of the statistical uniaxial model can be used at the third step by incorporating the computed nonlinear constitutive behaviour into finite element analyses, representing the stress–strain relation normal to the cracks.

The objective of this study was to develop a fairly general model, which includes both a single fracture and multiple cracking. If the crack spacing is higher than the fibre length, the stress–crack width relation represents a single fracture. Fibre orientation introduces additional phenomena, which include different fibre distributions, snubbing effect, and matrix spalling. Both these and hybrid composites are discussed, and are taken into account by describing their effects with simple mathematical models.

The model gives a complete constitutive relation (stress–strain or stress–crack width curve), which can further be used in finite element analyses. The proposed model is compared with experimental results found in the literature. The effects of fibre aspect ratio are also studied.

2. Macromechanical tensile behaviour

From the micromechanical properties it is possible to derive a model of a single fibre bridging one or several cracks [1, 2]. However, the result of a single-fibre analysis is not very practical for material design. It can be useful when studying the interaction between fibre and matrix, but usually the macromechanical properties are of greater interest. Moreover, the inclined fibres introduce additional phenomena, e.g. the number of fibres bridging the crack, pulley effect, and matrix spalling, which considerably affect the macromechanical behaviour. The macromechanical tensile behaviour can be derived by taking all fibres and their distribution into account. Only by means of a statistical analysis can the crack spacing, crack width, postcracking strength, and the ultimate strain be evaluated. Moreover, the behaviour of a hybrid composite is only possible by statistical analysis, because all fibre types must be considered for evaluation of the composite stress and when testing the condition of subsequent cracking.

Because non-linear behaviour is mainly due to cracking and the behaviour thereafter, the cracked stage is emphasized in this study. The composite is assumed to behave in linear elastic mode, up to the first crack strength. The elastic modulus of the uncracked composite is calculated using the rule of mixtures. Fibre length and orientation can be taken into account by efficiency factors.

Beyond the elastic limit, the crack is assumed to extend over the composite cross-section or, in finite element analysis, over the volume controlled by an integration point. Hence the crack is resisted only by the bridging fibres. The first crack strength is defined as the applied tensile stress at which the crack spreads throughout a cross-section. It depends on the fibre diameter, the fibre volume content, the moduli of the constituents, and the fracture energy of the matrix. Aveston *et al.* [3] derived the cracking strain of composites with continuous, aligned fibres. Li and Leung [4] stated the conditions for steady-state cracking and derived the first crack strength for discontinuous random fibre composites. Multiple cracking then takes place if the fibres are able to sustain a stress higher than the first crack strength. The matrix divides into segments, the length of which depends on the stress transfer from the fibres to the matrix. Cracking is observed to happen at a nearly constant stress. After the multiple cracking process, no further cracks form, and the composite shows strain-hardening behaviour until the fibres rupture or pull out.

2.1. Model requirements

The following requirements are set for the new constitutive model.

1. The composite may fail either in single fracture or in multiple cracking mode.
2. No restriction of fibre length is imposed.
3. No restriction of fibre volume content is imposed.
4. No restriction of fibre orientation is imposed.
5. Full bond, gradual debonding, and frictional bond are taken into account.
6. Fibres can pull out, break, or yield.
7. The composite may include several types of fibre (hybrid composite).
8. The result should include the stress–strain curve, the stress–crack width curve, and a prediction of crack spacing.

Conditions 2 and 3 may cause numerical problems, if the fibre length or the volume content is high. Moreover, the single-fibre analysis may lead to inaccurate results with very high fibre contents [1]. Without these limitations, the theory does not violate those conditions. For continuous fibres the model was slightly modified to assume equal forces in the fibre at the cracks. With the modified theory, however, fibre pull-out cannot be modelled nor the contribution of beaten fibres taken into account.

2.2. Assumptions

The following assumptions for the model are adopted.

1. Fibres are separate, straight and smooth.
2. Fibres are fully flexible in bending.
3. Both the fibres and the bulk matrix behave in linear elastic fashion up to their tensile strength.
4. The constitutive behaviour of the interface at the different stages is as follows.

(i) A linear relationship between the interface shear stress and the relative displacement of the fibre and the matrix in a full bond stage.

(ii) Debonding once the interfacial shear stress exceeds a threshold value.

(iii) Constant or decaying frictional shear stress along the debonded length.

5. Matrix cracks are planar and perpendicular to the load.
6. Matrix cracks form if the average stress in the matrix halfway between cracks exceeds the matrix cracking strength.
7. Several cracks form simultaneously, dividing the crack spacing in half.
8. Matrix spalling at the fibre exit from the matrix at an oblique angle is considered geometrically from a predefined spalled length.
9. Residual stresses caused by thermal or other mismatches are neglected.

Assumption 1 restricts the use of the model to straight and smooth fibres. However, fibres with a surface treatment or hooked ends are widely used because of their better anchorage. The model does not take their different mechanisms into account. The increased pull-out energy can be taken into account by changing the interfacial properties, which only approximates the true pull-out curve. The enhanced properties of the deformed fibres have been studied experimentally by Naaman and Najm [5] and theoretically by Chanvillard [6].

Assumption 2 means that the fibre acts like a rope, carrying only uniaxial stresses. No bending or shear stresses are taken into account. If the fibre aspect ratio is high, the assumption is justified. Leung and Li [7] studied numerically the fibre bending and matrix spalling mechanism, treating the fibre as a beam on an elastic foundation. The spalling criterion was also derived from the finite element analysis. However, because the bending energy is neglected in the present study, possible fibre breakage due to bending or shearing is not taken into account. Moreover, the spalling condition is not included but its effect can be taken into account if the spalled length is known (Assumption 8).

Fibre rupture or yielding and matrix cracking are considered the main causes of non-linear behaviour of the constituents. Therefore, the behaviour can be treated as linear elastic, up to a certain stress. However, some fibres may undergo extensive yielding prior to fibre rupture, e.g. polypropylene networks [8]. In that case, the model should be used with caution. The interfacial behaviour is elastic due to full bond until the interfacial shear strength is exceeded and debonding begins. Debonding may exhibit a gradual softening behaviour if the debonding energy, G_{II}, is relatively high [9]. Therefore, the interfacial frictional shear stress can be a decaying function.

In this study, only macrocracks are studied. Experiments have shown that the crack orientation is perpendicular to the tensile loading axis both in the case of aligned fibres and fibres in a random three-dimensional distribution ([10] Fig. 11). However, the assumption may not be valid in the case of fibres lying at a high angle to the loading, in which case the crack plane may be deflected parallel to the fibre–matrix interface [11].

In an average sense, the maximum stress in the matrix occurs halfway between the cracks. The stress state is only checked in that position. However, in the case of a high fibre inclination, a local stress at the fibre bending point may be high enough to cause matrix splitting. The condition of matrix spalling is a topic for future study.

Equal crack spacings and simultaneous formation of several cracks (Assumption 7) are merely to reduce the computational time. This assumption does not restrict the validity of the model. In the multiple cracking process, consider cracks to form one at a time. The load drops but reaches the cracking stress again, causing the subsequent crack to form. This process continues until the composite is divided into segments of equal length. The crack spacing predicted is not unique but falls somewhere between x' and $2x'$, where x' is the minimum crack spacing [3]. To obtain the minimum crack spacing, an iterative computation would be needed.

The residual stresses may be important, because they affect the cracking stress [12]. Moreover, they have a strong influence on inelastic strains and hysteresis [13]. Hsueh [14] showed that the axial residual stress strongly affects the fibre force required to debond the interface. Fibre sliding due to residual stresses was studied by Hsueh [15]. The methods for derivation of residual stress from experiments were suggested by Hsueh [16] and Hild *et al.* [13]. In order to include residual stresses, the theory in Part I [1] should be refined.

2.3. Fibre orientation

In Part I of this study [1], crack bridging by a single fibre was studied assuming the fibre to be located perpendicular to the crack. However, the fibres may be randomly distributed within the matrix, or may favour certain angles. If the assumption of flexible fibres in bending is made, the theory of aligned fibres can be used with minor modifications.

The effects of fibre inclination have been studied both experimentally, e.g. by Ouyang *et al.* [17] and Bartos and Duris [18], and theoretically, e.g. by Li [19], Stroven [20], and Jain and Wetherhold [21]. Bartos and Duris studied the effect of matrix spalling on the pull-out curve of inclined fibres. In most theoretical studies, the fibre position at the crack is assumed to be perpendicular to the crack faces. This is justified unless matrix spalling takes place, which allows the inclined position of the fibre at the crack [18]. The effect of matrix spalling is studied in the next section.

In the present section, matrix spalling is neglected for illustrative reasons. The main assumption concerning the fibre orientation throughout this study is that the fibre is completely flexible in bending, carrying only tensile stress.

The fibre orientation factor for the evaluation of composite stress can be derived for a single fracture mode, or if the crack spacing is higher than the fibre length. However, if the crack spacing is less than the fibre length, the fibre inclination leads to a change in the geometry because the crack spacing in the direction of an inclined fibre is

$$l = \frac{2s}{\cos\theta} \tag{1}$$

where $2s$ is the crack spacing, and θ is the inclination angle between the fibre and the direction normal to the crack.

Wang *et al.* [22] derived the fibre orientation factor η_θ, using the probability for a fibre to intercept the crack plane as a function of θ. For a random three-dimensional distribution, the factor was determined to be $\eta_\theta = 1/2$. Kullaa [23] extended the analysis to a subspace with the fibre inclination angle between θ_1 and θ_2. Moreover, separate formulae were derived for two- and three-dimensional subspaces. The results agree with the literature, resulting in factors of $\eta_\theta = 1/2$ and $\eta_\theta = 2/\pi$ for random three- and two-dimensional distributions, respectively, as well as $\eta_\theta = \cos\theta$ for parallel fibres.

As suggested by Li [4], the increased pull-out load of inclined fibres can be taken into account by modelling the fibre bending point as a pulley, with a snubbing friction coefficient, μ

$$\sigma_f = \sigma_f' e^{\mu\theta} \tag{2}$$

where σ_f' is the tensile stress in the inclined fibre inside the matrix, and σ_f the tensile stress in the fibre at the crack (see Fig. 1a). The average fibre stress can be obtained by integration

$$\overline{\sigma_f} = \frac{1}{A}\frac{2}{l_f}\int_0^{l_f/2}\left[\int_A \sigma_f'(l,\theta)\, e^{\mu\theta}\cos\theta\, \mathrm{d}A\right]\mathrm{d}l \tag{3}$$

where A depends on the fibre distribution (see the Appendix).

The average matrix force perpendicular to the crack transferred along the fibre length is

$$\bar{T} = \frac{1}{A}\frac{2}{l_f}\int_s^{s+l_f/2}\left[\int_A T(l,\theta)\cos^2\theta\, \mathrm{d}A\right]\mathrm{d}l \tag{4}$$

where T is the matrix force in the fibre direction and refers either to a force at a certain location or the average force within the matrix segment. In addition to Equation 4, an additional force is transferred at the fibre bending point (Fig. 1a). The average of this additional force is

$$\overline{P_{aux}} = \frac{1}{A}\frac{2}{l_f}\int_s^{s+l_f/2}\left[\int_A P(l,\theta)\,(e^{\mu\theta}-\cos\theta)\cos\theta\, \mathrm{d}A\right]\mathrm{d} \tag{5}$$

where P is the force in the inclined fibre at the crack. It should be noted that the direction of the additional force is perpendicular to the crack plane. Hence it is not transferred to the area A_m around the inclined fibre, but rather as an external force to the composite. Therefore, it is assumed that the matrix proportion of the force is

$$\overline{T_{aux}} = \frac{Q-1}{Q}\bar{P}_{aux} \tag{6}$$

where $Q = 1 + A_m E_m / A_f E_f$.

2.4. Matrix spalling

Matrix spalling may occur due to local stresses at the fibre bending point. If spalling occurs, it affects the inclined position of the fibre at the crack. Therefore, the fibre force component perpendicular to the crack is lower than that without matrix spalling (see Fig. 1). Moreover, the risk of fibre rupture due to bending decreases as the bending angle at the exit point decreases. On the other hand, the crack width and hence the strain become higher because of the altered geometry (see Fig. 2).

Let the crack width be w and the spalled length l_{sp} (Fig. 2). Owing to matrix spalling, the crack width consists of two components, one due to the fibre inclination, or the geometric change, and the other due to the pull-out. Let the pull-out component be w_{sp}. It is always less or equal to that without matrix

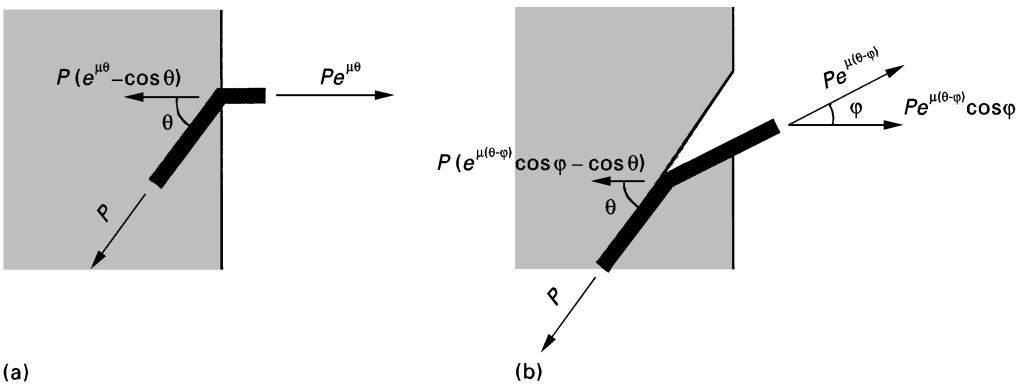

Figure 1 Forces at the crack due to fibre inclination and matrix spalling. (a) No matrix spalling, (b) matrix spalling included.

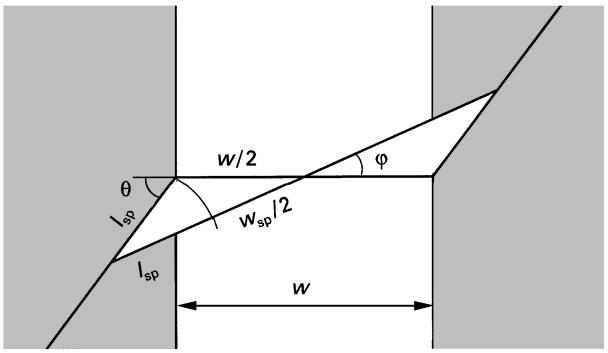

Figure 2 Geometry of a fibre bridging a crack at an oblique angle due to matrix spalling.

spalling and can be calculated by

$$w_{sp} = 2\{[(\tfrac{1}{2}w + l_{sp}\cos\theta)^2 + (l_{sp}\sin\theta)^2]^{1/2} - l_{sp}\} \quad (7)$$

The fibre orientation at the crack is

$$\varphi = \overline{\arctan}\,\frac{l_{sp}\sin\theta}{w/2 + l_{sp}\cos\theta} \quad (8)$$

The spalled length is still to be determined. Leung and Li [24] studied the coupled fibre bending/matrix spalling mechanism using the finite element method. They concluded that the spalled length depends on the fibre angle and the crack width. Within the crack-width region of their study, the relationship between the spalled length and the crack width was nearly linear. The dependence on the fibre angle was not too pronounced. Therefore, it would be justified to use a simple relationship for the spalled length

$$l_{sp} = kw \quad (9)$$

where the coefficient k is to be determined from experiments or finite element analyses. For fixed fibre inclination, θ, Relationship 9 leads to a constant fibre angle φ at the crack, independent of the crack width. This may not be realistic, at least at high crack widths, because the angle φ probably decreases with an increasing crack width. The slopes k in Leung and Li's study [24] were seen to decrease with increasing crack width, and may possibly have reached a limit at higher crack widths. Therefore, another simple model with a constant spalled length would be more realistic, at least at higher crack widths. A criterion for matrix spalling and an estimation of the spalled length are yet to be developed.

When the fibre inclination φ is known, the force components for the composite analysis can be evaluated and are shown in Fig. 1b. It should be remembered that the fibres are assumed to carry tensile loads only. Taking matrix spalling into account, the composite stress and the additional force at the bending point (cf. Equations 3 and 5, respectively) become

$$\overline{\sigma_f} = \frac{1}{A}\frac{2}{l_f}\int_0^{l_f/2}\left[\int_A \sigma_f'(l,\theta)^{\mu(\theta-\varphi)}\cos\varphi\cos\theta\,dA\right]dl \quad (10)$$

$$\bar{P}_{aux} = \frac{1}{A}\frac{2}{l_f}\int_s^{s+l_f/2}\left[\int_A P(l,\theta)\,(e^{\mu(\theta-\varphi)}\cos\varphi - \cos\theta)\cos\theta\,dA\right]dl \quad (11)$$

Equations 10 and 11 take into account the fibre distribution, the pulley effect, and matrix spalling. It can be seen that the pulley effect increases the fibre stress, while matrix spalling has the opposite effect.

2.5. Crack localization

Beyond peak stress in multiply-cracked composites, the stress decreases causing strain-softening, or crack localization. This means that one crack opens while the others close. In this process two constitutive relations can be distinguished, the stress–strain curve and the stress–crack width curve. The former consists of the crack widths equal to all of the closing cracks as well as the strain in the matrix. The latter consists of the additional crack width of the opening crack. In finite element analysis, these two constitutive relations should be distinguished.

The analysis is as follows. It is assumed that a certain proportion of the crack width is permanent. The width of the opening crack is increased gradually while the others are closing. Aveston *et al.* [3] derived a value for the permanent strain after unloading. Hild *et al.* [13] studied unloading and the corresponding hysteresis up to the strain where debonding extends through the matrix segment. Beyond that point, their theory is not valid. A more robust model for crack localization and unloading is still to be developed, which would result in the theoretical permanent crack opening, without the need to predefine it. The present model is presumed to be accurate enough for the purposes mentioned earlier.

2.6. Hybrid composite

Very few models for hybrid composites are available. Kakemi and Hannant [8] developed a mathematical model for a hybrid composite with two types of continuous aligned fibres and a pure frictional bond. In the following, a theory is developed which can include more than two types of fibre, all of which may have different properties and distribution.

To obtain the matrix area occupied by a single fibre of type i, let us examine a representative volume element of the composite with n different fibre types. Assume the fibres to be aligned, and study the cross-sectional area A_c of the element. The total fibre volume content is

$$V_f = \sum_{i=1}^{n} V_f^i = \frac{1}{A_c}\sum_{i=1}^{n} N^i A_f^i = \frac{V_m}{A_m}\sum_{i=1}^{n} N^i A_f^i \quad (12)$$

where N^i is the number of fibres of type i. A_m is the total matrix area within A_c, and can be derived from 12

$$A_m = \frac{V_m}{V_f}\sum_{i=1}^{n} N^i A_f^i \quad (13)$$

On the other hand, if A_m^i is the matrix area occupied by a single fibre of type i, the total matrix area can be written as

$$A_m = \sum_{i=1}^{n} N^i A_m^i \quad (14)$$

Combining Equations 13 and 14, and recognizing that N^i can be arbitrary, leads to

$$A_m^i = \frac{V_m}{V_f} A_f^i \tag{15}$$

To compute for the tensile stress in the matrix due to the force transferred from fibres of type i, the force must be divided by a total matrix area A_m. From Equation 12 and the fact that N^i can be arbitrary, the total matrix area is

$$A_m = \frac{V_m}{V_f^i} N^i A_f^i \tag{16}$$

On the other hand, when analysing one fibre type at a time, the force from a fibre is transferred to a matrix area $\hat{A}_m^i$, and the area A_m can be written as

$$A_m = N^i \hat{A}_m^i \tag{17}$$

Finally, combining Equations 16 and 17, the matrix area for a single fibre of type i for matrix stress calculation is

$$\hat{A}_m^i = \frac{V_m}{V_f^i} A_f^i \tag{18}$$

The areas A_m^i and $\hat{A}_m^i$ in Equations 15 and 18 are mutually equal if a single fibre type is analysed.

2.7. Stress and strain

The final step from a single fibre analysis to the composite constitutive relationship is to compute the stresses and strains. The composite stress can be obtained from the stresses in the fibres at the crack by

$$\sigma_c = \sum_{i=1}^{n} V_f^i \overline{\sigma_f^i} \tag{19}$$

where $\overline{\sigma_f^i}$ is given by Equation 3. The composite strain during the strain hardening in the multiply-cracked stage is

$$\varepsilon_c = \overline{\varepsilon_m} + \frac{w}{2s} = \sum_{i=1}^{n} \frac{1}{\hat{A}_m^i E_m} \left[\overline{T^i(x)} + \overline{T_{aux}^i} \right] + \frac{w}{2s} \tag{20}$$

To check for matrix cracking, the average matrix strain at the middle of the segment is obtained by multiplying $\overline{\varepsilon_m}$ by E_m

$$\overline{\sigma_m(s)} = \sum_{i=1}^{n} \frac{1}{\hat{A}_m^i} \left[\overline{T^i(s)} + \overline{T_{aux}^i} \right] \tag{21}$$

It should be noted that the aggregate bridging stress, σ_m^a [25], is not taken into account. It can be simply included by summing an additional term $V_m \sigma_m^a$ to the stress in Equation 19 and a term $V_m \sigma_m^a / E_m$ to the composite strain in Equation 20. Strictly speaking, the additional stress causes different boundary conditions in the fibre analysis at the cracks [1]. The effect of aggregate bridging occurs only with low crack widths. Therefore, its influence on the total stress–strain curve is negligible at higher strains.

2.8. Calculation procedure

Computation of the constitutive relationship is performed according to the following algorithm. The starting point for the calculation is a large crack spacing and zero crack width. The crack width is gradually increased. At every crack width, the crack bridging analysis [1] is performed separately for all fibre types, fibre locations and orientations. The average fibre and matrix stresses are evaluated, and the matrix cracking criterion tested. If cracking takes place, the crack spacing is halved, and the calculation is started from the beginning at zero strain. Finally, the composite stress and strain are evaluated.

If the fibre length is much greater than the crack spacing, the computational time may become too long, because the number of equations in fibre analysis depend on the number of cracks bridged by a fibre, which increases as the crack spacing decreases. The fibre analysis is an iterative process, and is performed for every fibre location and orientation. In some examples, the integration was performed using 20 fibre location and 10 fibre angles. In the other examples, five fibre locations and angles were used.

3. Model verification

The proposed model was verified against the ACK theory by Aveston, Cooper, and Kelly [3, 26] and was seen to agree with it [27]. The ACK theory was originally developed for continuous, aligned fibres, but was later extended to evaluate the peak stress and the crack spacing of discontinuous and randomly oriented fibre composites. However, the fibre pull-out cannot be modelled with the theory, and moreover the analysis of hybrid composites is not included. Therefore, the proposed model can be considered as an extension of the ACK model.

In an internal report [27], parametric calculations were performed to study the effects of different micromechanical parameters on the constitutive relationship. The parameters include the stiffness ratio of the fibre and the matrix, the fibre volume content, the fibre aspect ratio, the frictional shear stress, and the fibre orientation. The present paper studies the effect of fibre diameter.

Unfortunately, few experimental results are available for tensile specimens, which include discontinuous randomly oriented fibres, and which fail in the multiple cracking mode. The verification is made against an ECC material consisting of discontinuous polyethylene fibres, the failing mode being fibre pull-out.

The validity of the proposed model for analysing hybrid composites was also studied by Kullaa [27] compared with the experimental results by Kakemi and Hannant [8] and Xu and Hannant [28].

3.1. Effects of fibre diameter

The effect of fibre diameter is studied using the values $d = 1.0$, 0.5, 0.25, and 0.1 mm, and fibre aspect ratios $l_f/d = 40$, 80, 160, and 400, respectively. The bond

modulus, κ, is inversely proportional to the fibre diameter [29], leading to values of $\kappa = 1.24 \times 10^{13}$, 2.48×10^{13}, 4.96×10^{13}, and $1.24 \times 10^{14}\,\mathrm{N\,m^{-3}}$, respectively. The other micromechanical parameters are: for the matrix, modulus of elasticity $E_m = 21\,\mathrm{GPa}$, and cracking stress $\sigma_{mu} = 5\,\mathrm{MPa}$; for fibres, modulus of elasticity $E_f = 210\,\mathrm{GPa}$, volume fraction $V_f = 5\%$, length $l_f = 40\,\mathrm{mm}$, and tensile strength $\sigma_{fu} = 1000\,\mathrm{MPa}$; for the interface, shear strength $\tau_u = 4.0\,\mathrm{MPa}$, and frictional shear stress $\tau_f = 3.0\,\mathrm{MPa}$. Fibres are distributed in a random three-dimensional array.

The stress–strain relationships are shown in Fig. 3. Composites with the two lowest aspect ratios fail with a single fracture mode. A characteristic length of 40 mm is chosen for plotting the strains. Composites with an aspect ratio larger than 400 fail in fibre rupture, all having equal post-cracking stiffnesses and strengths. Therefore, a further increase of the aspect ratio does not change the stress–strain relation. On the other hand, the crack spacing and crack width halve as the fibre aspect ratio doubles. Further cracking is predicted also at higher stresses, due to additional stresses at fibre bending points. The highest possible strength is achieved with a high fibre aspect ratio, but the ductility becomes low because of fibre rupture. An intermediate fibre aspect ratio is seen to lead to multiple cracking, as well as to high ductility and strength. This can be seen with a fibre aspect ratio of 160, resulting in a fibre pull-out failure mode. Therefore, the strain capacity is higher than that with an aspect ratio of 400 or more.

3.2. Engineered cementitious composite

Maalej and Li [30] studied a new strain-hardening material, called an engineered cementitious composite (ECC) with randomly oriented discontinuous polyethylene fibres. The material properties used in calculations are: for the matrix, modulus of elasticity $E_m = 21\,\mathrm{GPa}$, and cracking stress $\sigma_{mu} = 2.5\,\mathrm{GPa}$; for fibres, modulus of elasticity $E_f = 120\,\mathrm{GPa}$, volume fraction $V_f = 2\%$, diameter $d = 0.038\,\mathrm{mm}$, length $l_f = 12.7\,\mathrm{mm}$, and tensile strength $\sigma_{fu} = 2700\,\mathrm{MPa}$; for the interface, shear strength $\tau_u = 2.0\,\mathrm{MPa}$, frictional shear stress $\tau_f = 0.85\,\mathrm{MPa}$, and frictional snubbing coefficient $\mu = 0.7$.

The ultimate strain of the composite was seen to be as high as 5.5%, which is higher than the fracture strain of the fibre. To achieve such a high strain, some strain must be formed without stretching the fibres. This is possible if the matrix spalls at the fibre exit point. Two models for the matrix spalling length are compared, $l_{sp} = kw$, where k is chosen to be 0.5, and $l_{sp} = 0.001\,\mathrm{mm}$.

The experimental stress–strain curve is shown in Fig. 4. The computed curves are shown in Fig. 5. It can be seen that without modelling the matrix spalling, the ultimate strain is approximated too low. From the two models of matrix spalling, the constant spalled length seems to give results which are closer to the experimental curve at higher strains, while the linearly increasing spalled length agrees better with the experiments at low strains. This observation supports the discussion in Section 2.4. It should be noted, however, that matrix spalling is not reported in the cited study by Maalej and Li [30], although its existence

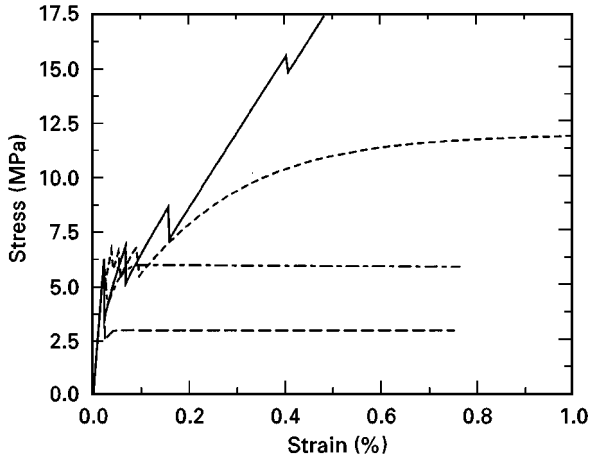

Figure 3 Computed constitutive relations for different fibre diameters d: (——) 0.1 mm, (– – –) 0.25 mm, (– – –) 0.5 m, (— — —) 1 mm.

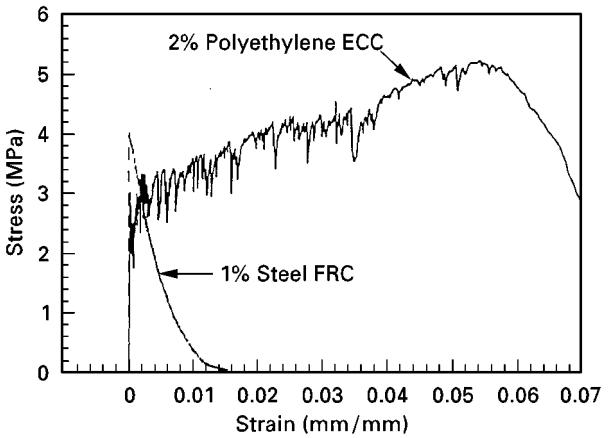

Figure 4 Experimental stress–strain curve for ECC [31].

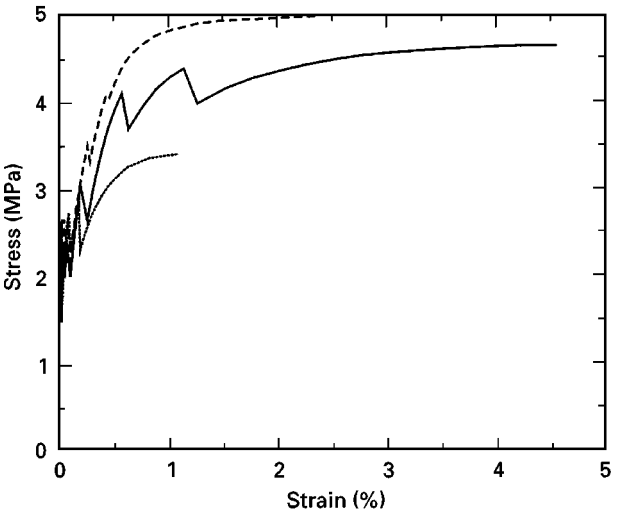

Figure 5 Computed stress–strain curves for ECC (– – –) Martix spalling not included, (· · · ·) spalled length $l_{sp} = 0.5w$, (——) $l_{sp} = 0.001\,\mathrm{mm}$.

can be deduced from a tension-softening curve in the earlier study by Ward and Li [32].

Because of snubbing, high forces are transferred into the matrix, and the crack spacing and the crack width tend to be very low. The computed crack spacing is less than 0.4 mm and the maximum crack width is 0.017 mm. Further cracking was not allowed, as this would have produced too many equations. However, the crack spacing of 0.4 mm is probably not realistic. If the crack spacing is lower, the spalled length of the matrix should be increased to obtain a high composite strain. For example, with a crack spacing of 1.6 mm, a spalled length of 0.006 mm leads to a strain of 6% and a crack width of 0.1 mm. A relatively high spalled length ($l_{sp} = 0.07$ mm) results in a more realistic crack spacing of 3.2 mm ([10], Fig. 11). Matrix spalling is more pronounced at high fibre angles. However, its dependence on the fibre angle is not taken into account in this study.

It is concluded that the behaviour of an ECC material can be reproduced from the micromechanical properties. The modelling of matrix spalling is essential for obtaining high strains and a realistic crack spacing as observed in experiments. The condition of matrix spalling is not included in the model, but the spalled length can be entered. A spalled length of only a fraction of the crack spacing increases considerably the strain capacity of the composite.

4. Conclusion

A statistical micromechanical model of multiple cracking is developed in which the statistical parameters are fibre orientation and fibre location. For every location and orientation, a fibre analysis is performed based on a two-fibre theory. The results of a fibre analysis include the fibre stress at the crack and the force in the matrix. These values are then averaged to obtain the stress and strain in the composite. In addition, the average matrix stress is evaluated for testing the cracking criterion.

Analysing fibres parallel to the loading is quite simple because of the few micromechanical parameters involved. Only the properties of the interface cannot be directly measured. Fibre orientation introduces additional micromechanical parameters which cannot be measured from a pull-out test of an aligned fibre. Such parameters include the snubbing frictional coefficient and the spalled length of the matrix, and a systematic experimental procedure is needed to measure them. The pulley effect increases the composite stress, whereas matrix spalling has the opposite effect. Moreover, the strain capacity of composites with randomly distributed fibres is considerably enhanced due to matrix spalling.

The constitutive relationships of fibre-reinforced brittle materials under uniaxial tensile load can be used as such to evaluate the tensile strength, crack width, crack spacing, or ultimate strain of the composite. Moreover, the effects of different material parameters can be studied by varying one parameter at a time and comparing the results. Hence the model is useful to a structural engineer as well as to a material designer. The derived constitutive relationships – either stress–strain, or stress–crack width curves – will later be used in numerical analyses to represent the behaviour normal to the crack. The smeared and discrete crack models make it possible to extend the present one-dimensional constitutive model to two and three dimensions. This will be the subject of future work.

Appendix. Fibres oriented in different subspaces

The following analysis is similar to that outlined by Kullaa [23], except for the additional snubbing term. The average fibre stress at the crack for a uniform distribution in a three-dimensional subspace between the angles θ_1 and θ_2 is

$$\overline{\sigma_f} = \frac{1}{\cos\theta_1 - \cos\theta_2}\frac{2}{l_f}\int_0^{l_f/2} \times\left[\int_{\theta_1}^{\theta_2} \sigma_f'(l,\theta)\, e^{\mu\theta}\sin\theta\cos\theta\,\mathrm{d}\theta\right]\mathrm{d}l \qquad \text{(A1)}$$

If σ_f' depends only on the fibre embedded length, as assumed in a single fracture mode, the integration in Equation A1 can be evaluated, leading to

$$\overline{\sigma_f} = \eta_\theta \frac{2}{l_f}\int_0^{l_f/2} \sigma_f'(l)\,\mathrm{d}l \qquad \text{(A2)}$$

where

$$\eta_\theta = \frac{e^{\mu\theta_2}(\mu\sin 2\theta_2 - 2\cos 2\theta_2) - e^{\mu\theta_1}(\mu\sin 2\theta_1 - 2\cos 2\theta_1)}{2(4+\mu^2)(\cos\theta_1 - \cos\theta_2)} \qquad \text{(A3)}$$

For a random uniform distribution ($\theta_1 = 0$, $\theta_2 = \pi/2$), Equation A3 gives

$$\eta_\theta = \frac{1 + e^{\mu\pi/2}}{4+\mu^2} \qquad \text{(A4)}$$

which is found to be twice the value of the snubbing factor g defined by Li [19]. Further, if the snubbing friction is zero, the orientation factor becomes $\eta_\theta = 1/2$. For an arbitrary three-dimensional fibre distribution, with zero snubbing friction the orientation factor becomes

$$\eta_\theta = \frac{\sin^2\theta_2 - \sin^2\theta_1}{2(\cos\theta_1 - \cos\theta_2)} \qquad \text{(A5)}$$

which is equal to that derived by Kullaa [23]. If the fibres are parallel at an angle θ, the orientation factor is derived by L'Hôpital's rule, leading to

$$\eta_\theta = e^{\mu\theta}\cos\theta \qquad \text{(A6)}$$

In a two-dimensional case, the average stress in the fibre is [23]

$$\overline{\sigma_f} = \frac{1}{\theta_2 - \theta_1}\frac{2}{l_f}\int_0^{l_f/2}\left[\int_{\theta_1}^{\theta_2} \sigma_f'(l,\theta)\, e^{\mu\theta}\cos\theta\,\mathrm{d}\theta\right]\mathrm{d}l \qquad \text{(A7)}$$

If σ_f' depends only on the fibre embedded length, the integration in Equation A7 becomes Equation A2, with

$$\eta_\theta = \frac{e^{\mu\theta_2}(\mu\cos\theta_2 + \sin\theta_2) - e^{\mu\theta_1}(\mu\cos\theta_1 + \sin\theta_1)}{(1+\mu^2)(\theta_2 - \theta_1)} \quad \text{(A8)}$$

For a random uniform two-dimensional distribution ($\theta_1 = 0$, $\theta_2 = \pi/2$), Equation A8 gives

$$\eta_\theta = \frac{2(e^{\mu\pi/2} - \mu)}{\pi(1+\mu^2)} \quad \text{(A9)}$$

Further, if the snubbing friction is zero, the orientation factor becomes $\eta_\theta = 2/\pi$. For an arbitrary two-dimensional fibre distribution, with zero snubbing friction the orientation factor becomes

$$\eta_\theta = \frac{\sin\theta_2 - \sin\theta_1}{\theta_2 - \theta_1} \quad \text{(A10)}$$

which is equal to that derived by Kullaa [23]. If the fibres are parallel at an angle θ, the orientation factor is derived by L'Hôpital's rule, leading to Equation A6.

However, the three-dimensional formulae are only valid for distributions symmetrical to the crack plane. For a more general fibre distribution, it is assumed that the fibre ends are distributed over a segment of a sphere (Fig. A1). The segment is at an angle α from the crack plane. The probabilistic density is [22]

$$p(\theta) = \frac{1}{A}\frac{dA}{d\theta} \quad \text{(A11)}$$

where A is the surface area of the hemisphere with radius l, l being the fibre embedded length. In this case the analysis leads to

$$A = 2\pi l^2[1 - \cos\tfrac{1}{2}(\theta_2 - \theta_1)] \quad \text{(A12)}$$

$$dA = \varphi l^2 \sin\theta\, d\theta \quad \text{(A13)}$$

where φ can be derived from the following equations

$$\cos\frac{\varphi}{2} = 1 - \frac{h/\sin\alpha}{l\sin\theta} \quad \text{(A14)}$$

$$h = \min[l\cos(\theta - \alpha) - y_s,\ 2l\sin\theta] \quad \text{(A15)}$$

$$y_s = l\cos\tfrac{1}{2}(\theta_2 - \theta_1) \quad \text{(A16)}$$

Finally, the average fibre stress can be obtained from Equation 3, which must now be integrated numerically.

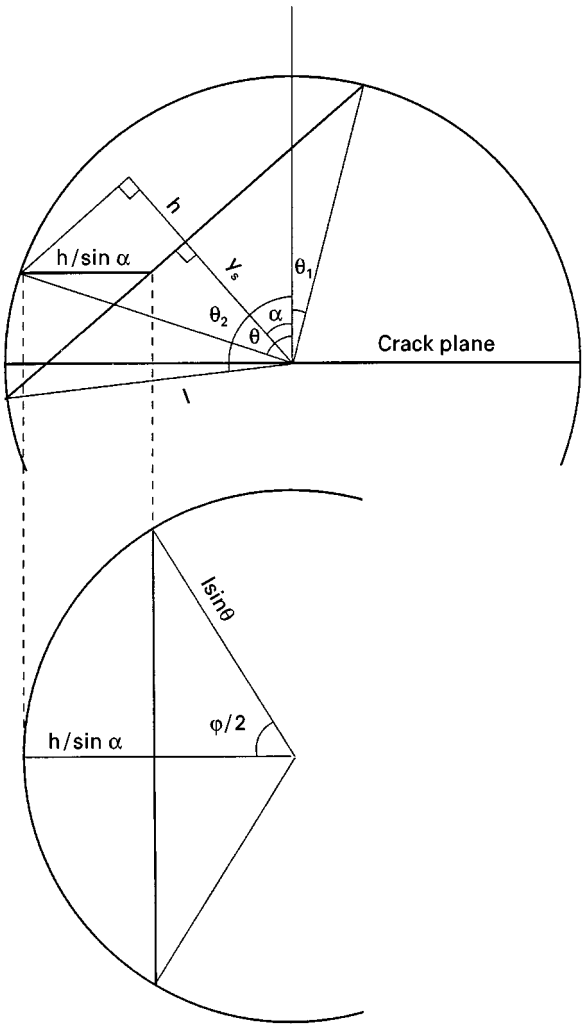

Figure A1 Fibre distribution in a three-dimensional subspace between angles θ_1 and θ_2. l is the fibre embedded length.

Acknowledgements

This study was carried out in the Netherlands, at Delft University of Technology, Faculty of Civil Engineering, and at TNO Building and Construction Research as part of a European Community research training project "Constitutive modelling of fibre-reinforced brittle materials for numerical analysis" under the programme "Training and Mobility of Researchers" financed by the European Commission.

References

1. J. KULLAA, *J. Mater. Sci.* **33** (1998) 0000.
2. *Idem*, *ibid.* **31** (1996) 61.
3. J. AVESTON, G. A. COOPER and A. KELLY, in "Single and multiple fracture. The Properties of Fibre Composites", Proceedings of a Conference National Physical Laboratories. (IPC Science and Technology, Guildford, 1971) pp. 15–24.
4. V. C. LI and C. K. Y. LEUNG, *J. Eng. Mech.* **118** (1992) 2246.
5. A. E. NAAMAN and H. NAJM, *ACI Mater. J.* **88** (2) (1991) 135.
6. G. CHANVILLARD, in Proceedings of the International Symposium "Brittle Matrix Composites 4", edited by A. M. Brandt, V. C. Li and I. H. Marshall (Ike and Woodhead, Warsaw, 1994) pp. 311–19.
7. C. K. Y. LEUNG and V. C. LI, *J. Mech. Phys. Solids* **40** (1992) 1333.
8. M. KAKEMI and D. J. HANNANT, *Composites* **26** (1995) 637.
9. Z. P. BAŽANT and R. DESMORAT, *J. Eng. Mech.* **120** (1994) 1945.
10. V. C. LI, Proceedings of the International Symposium "Brittle Matrix Composites 4", edited by A. M. Brandt, V. C. Li and I. H. Marshall (Ike and Woodhead, Warsaw, 1994) pp. 63–80.
11. V. C. LI, Y. WANG and S. BACKER, *J. Mech. Phys. Solids.* **39** (1991) 607.
12. B. BUDIANSKY, J. W. HUTCHINSON and A. G. EVANS, *ibid.* **34** (1986) 167.
13. F. HILD, A. BURR and F. A. LECKIE, *Int. J. Solids Struct.* **33** (1996) 1209.
14. C.-H. HSUEH, *Mater. Sci. Eng.* **A145** (1991) 135.
15. *Idem*, *ibid.* **A145** (1991) 143.
16. *Idem*, *Acta Metall. Mater.* **38** (1990) 403.

17. C. OUYANG, A. PACIOS and S. P. SHAH, *J. Eng. Mech.* **120** (1994) 2641.
18. P. J. M. BARTOS and M. DURIS, in Proceedings of the International Symposium "Brittle Matrix Composites 4", edited by A. M. Brandt, V. C. Li, and I. H. Marshall (Ike and Woodhead, Warsaw, 1994) pp. 320–31.
19. V. C. LI, *J. Mater. Civil Eng.* **4** (1992) 41.
20. P. STROEVEN, Proceedings of the International Symposium "Brittle Matrix Composites 4", edited by A. M. Brandt, V. C. Li and I. H. Marshall (Ike and Woodhead, Warsaw, 1994) 301–10.
21. L. K. JAIN and R. C. WETHERHOLD, *Acta Metall. Mater.* **40** (1992) 1135.
22. Y. WANG, S. BACKER and V. C. LI, *Composites* **20** (1989) 265.
23. J. KULLAA, *Composites* **25** (1994) 935.
24. C. K. Y. LEUNG, *J. Eng. Mech.* **118** (1992) 2298.
25. V. C. LI, H. STANG and H. KRENCHEL, *Mater. Struct.* **26** (1993) 486.
26. J. AVESTON, R. A. MERCER and J. M. SILLWOOD, "Fibre reinforced cements-scientific foundations for specifications. Composites-standards, testing and design", Proceedings, National Physical Laboratory (IPC Science and Technology Press, Guilford, 1974) pp. 93–103.
27. J. KULLAA, "Micromechanics of multiple cracking. Statistical tensile behaviour", TUD report 03.21.0.22.21, Delft University of Technology, Faculty of Civil Engineering, Delft (1996) 54 p.
28. G. XU and D. J. HANNANT, *Cement Concr. Compos.* **13** (1991) 95.
29. J. KULLAA, *J. Struct. Eng.* **122** (1996) 783.
30. M. MAALEJ and V. C. LI, *ACI Struct. J.* **92** (1995) 167.
31. M. MAALEJ and V. C. LI, *J. Mater. Civil Eng.* **6** (1994) 513.
32. R. WARD and V. C. LI, *ACI Mater. J.* **87** (1990) 627.

Received 21 February 1997
and accepted 15 May 1998